Water Supply

IWA PUBLISHING

Water Supply Vol 22 No 3, 2816 doi: 10.2166/ws.2021.436

Modeling the supply, demand, and stress of water resources using ecosystem services concept in Sirvan River Basin (Kurdistan-Iran)

Jahanbakhsh Balist[a,*], Bahram Malekmohammadi[a], Hamid Reza Jafari[a], Ahmad Nohegar[a] and Davide Geneletti[b]

[a] School of Environment, College of Engineering, University of Tehran, Tehran, Iran
[b] Department of Civil, Environmental and Mechanical Engineering, University of Trento, Via Mesiano 77, 38123, Trento, Italy
*Corresponding author. E-mail: j.balist@ut.ac.ir

BM, 0000-0002-3964-7536

ABSTRACT

Water resources modeling can provide valuable information to planners. In this respect, water yield is an ecosystem service with significant roles in the sustainability of societies and ecosystems. The present study aimed to model the supply and demand of water resources and identify their scarcity and stress in the Sirvan river basin. For this purpose, we employed the ecosystem services concept as new thinking in earth sciences and using soil, climate, and land use data. Firstly, the Landsat satellite images of 2019 were prepared after different corrections, and the land use map was produced. Then, precipitation, evapotranspiration, root restricting layer depth, and evapotranspiration coefficients of the land uses were prepared and modeled in the InVEST 3.8.9 software environment. The findings indicated that the water yield in this river basin is 5,381 million m^3, with sub-basins 5, 11, and 1 having the highest water yield per year and sub-basin 2 having the lowest water yield. Moreover, sub-basins 5 and 11 had the highest water consumption. Based on the estimated water scarcity and stress index, sub-basin 8 has experienced water scarcity and sub-basin 4 water stress. We conclude that applying the InVEST Water Yield model to assess water resource status at the basin and sub-basins level can provide suitable results for planning.

Key words: ecosystem services, Sirvan river basin, water resources, water stress

HIGHLIGHTS

- Accurate knowledge of the status of water resources, including supply and demand at the basins, is a key requirement in water managing and planning.
- Factors of population growth, population displacement must be considered in modeling and planning.
- Using water scarcity and stress index in water resources management at the basin level can bring about stability in the supply and demand of ecosystem services and conservation.

INTRODUCTION

Water resources are increasingly under pressure due to different pressures like climate change, population growth, declining groundwater, increasing energy demand, and environmental water requirements (Touch *et al.* 2020). Water is a vital natural resource, especially in arid and semi-arid regions of the world. It is essential for balancing socio-economic development and ecological security and is, therefore, a vital issue for water resources management. The water resources provided by precipitation and snowfall in the region are highly changeable and vulnerable to many factors, including climate change (Yang *et al.* 2020). Water scarcity has become a significant constraint on socio-economic development and a menace to livelihoods in several parts of the world (Liu *et al.* 2017). Concerns over water scarcity and its over-exploitation are increasing because of economic growth and the increase in demand for food and biofuels (Zhang *et al.* 2013; Gheewala *et al.* 2014; Baloch *et al.* 2015; Gheewala *et al.* 2018). The World Economic Forum reports that water stress is one of the greatest threats today. Thus, there is an indispensable need to solve water stress problems (Wang *et al.* 2021a). In this regard, the development of a water stress index is essential to evaluate the status in various areas (Uche *et al.* 2015; Gheewala *et al.* 2018). In recent years, ecosystem services have been increasingly used worldwide in decision-making, especially in the field of water resources (Cabral *et al.* 2021).

Ecosystem services are the advantages humans get from ecosystems and include provisioning, regulatory, supportive, and cultural services (Yang *et al.* 2021). However, economic development usually leads to the destruction of ecosystem services (Costanza *et al.* 2014). In 2018, the United Nations proposed the sustainable development goals to balance social development conflicts and ecosystem services (2018). Aquatic ecosystems support the provision of essential ecosystem services like fish production, water supply, and recreation. Ecosystem services are associated with the hydrological cycle in the river basin (Grizzetti *et al.* 2016). With water scarcity, hydrological ecosystem services have turned into a hot topic in ecosystem management (Chen *et al.* 2015). As a key component of hydrological ecosystem services, producible water has a vital role in ecosystem management and hydrological equilibrium (Brauman 2015; Zou & Mao 2021). Evaluating the changes in water yield ecosystem services in response to land use and climate change is a practical approach to evaluate land use planning costs and environmental resources. Hence, modeling the ecosystem services of the water yield of a basin can be effective in managing the monitoring and predicting the effects of economic development policies and the consequences of land-use change for proper planning (Lang *et al.* 2017).

Water supply is controlled directly by precipitation and evapotranspiration and indirectly by the land use (Bonan 2015; Sun *et al.* 2018). Climate affects water supply by changing the precipitation pattern in basins (Yang *et al.* 2021). On the other hand, the consumption uses of water resources are chiefly divided into agricultural, industrial, domestic, and ecological water. The amount of domestic water directly affects the quality of life of residents. The predicted value of household water consumption can be used as a significant reference index for water supply decision-making and the basis for expressing water supply and drainage planning and national economic planning (Wang *et al.* 2021b). In addition, the land use affects the water supply and water quality by changing the ground level of basins (Lang *et al.* 2017; He & Wu 2019; He *et al.* 2019). Many studies have been carried out to examine the effects of climate and land use on basins water supply (Zhang *et al.* 2013; Pessacg *et al.* 2015). Nonetheless, few studies have considered the simultaneous effect of climate and land use on water supply.

Many models have been developed to estimate water yield at the basin level at different types. For example, the Integrated Valuation of Ecosystem Services and Tradeoffs (InVEST) model was developed as a part of the Natural Capital Project, whose purpose was to align economic objectives with conservation objectives and mainstream approaches. Evaluation via InVEST water yield model can be used to estimate the relative share of water yield from various basin regions and determine the effect of different land covers on annual water yield and its spatial distribution (Chacko *et al.* 2019).

Different studies have examined the effects of climatic and land use parameters on water yield. The results have shown a positive correlation between precipitation and water yield (Pessacg *et al.* 2013) and various relationships between land use and water yield (Li *et al.* 2018; Zhang *et al.* 2018). For instance, Redhead and Stratford validated the InVEST water yield model in various basins in England. Also, they analyzed the model through various sensitization inputs (Redhead *et al.* 2016). Yin *et al.* conducted a sensitivity analysis on a water yield model based on climatic parameters (Yin *et al.* 2020). In this regard, InVEST is a suitable spatial tool of open-source models to design and quantify natural resource ecosystem services (Sharp *et al.* 2019). Some studies have validated the effectiveness of the InVEST model in estimating the ecosystem services of different ecosystems (e.g Bouguerra & Jebari 2017; Sallustio *et al.* 2017; Haiping *et al.* 2018).

As one of the Tigris sub-basins, the Sirvan river basin has a high potential for water yield in the region. However, due to mismanagement, this valuable resource has many problems in land use planning and, consequently, economic and livelihood problems of the people. Moreover, the environment of the region has experienced extensive degradation due to the inter-basin transfer of water. Hence, it is essential to know the status of water resources in this basin.

The study attempts to estimate the water yield in the Sirvan river basin quantitatively using the water yield model in the InVEST software environment. Moreover, the water demand and consumption are estimated based on the land use type and population. The amount of water yield in the basin and sub-basins is calculated based on climatic parameters such as precipitation and evapotranspiration, soil condition of the region like root restricting layer depth, and land use. Moreover, the status of water resources in the sub-basins is evaluated based on the water scarcity and stress index. These indices in evaluating the water status in the region can be used to plan water resources in the future.

MATERIALS AND METHODS

Description of the study area

Sirvan river basin with an area about 13,400 km^2 is located between 45° 59′ to 47° 22′ East and 34° 50′ to 35° 05′ North (northern and eastern hemisphere) (Peyman *et al.* 2020; Yariyan *et al.* 2020; Balist *et al.* 2022) covering parts of the Kurdistan and Kermanshah provinces of Iran. This basin contains 11 sub-basins (Figure 1). Sirvan is an important river in the western border basin, collecting the waters of large western Iran waters and entering the Persian Gulf after entering Iraq and joining the Tigris River. This river flows in Kurdistan and Kermanshah, Sanandaj, Marivan, Paveh, Nosud, and Javanroud being in its river basin. Also, a population of one million people lives in this basin. Climatic information of the region is given in Table 1. The soil of the study area includes Rock Outcrops/Entisols with 66%, Rock Outcrops/Inceptisols with 18%, Entisols/Inceptisols with 2%, Inceptisols with 13%, and Inceptisols/Vertisols with 1%. Soil texture varies mainly from heavy to relatively heavy and in three primary soils: clay, loamy clay, and loam.

Field data collection

The data used in this study include land use, climatic parameters (precipitation, evaporation, and transpiration), plant available water content, root restricting layer depth, evapotranspiration coefficient of various land cover, and root depth (Table 2).

Model description

The process used in the study is presented as a flowchart in Figure 2.

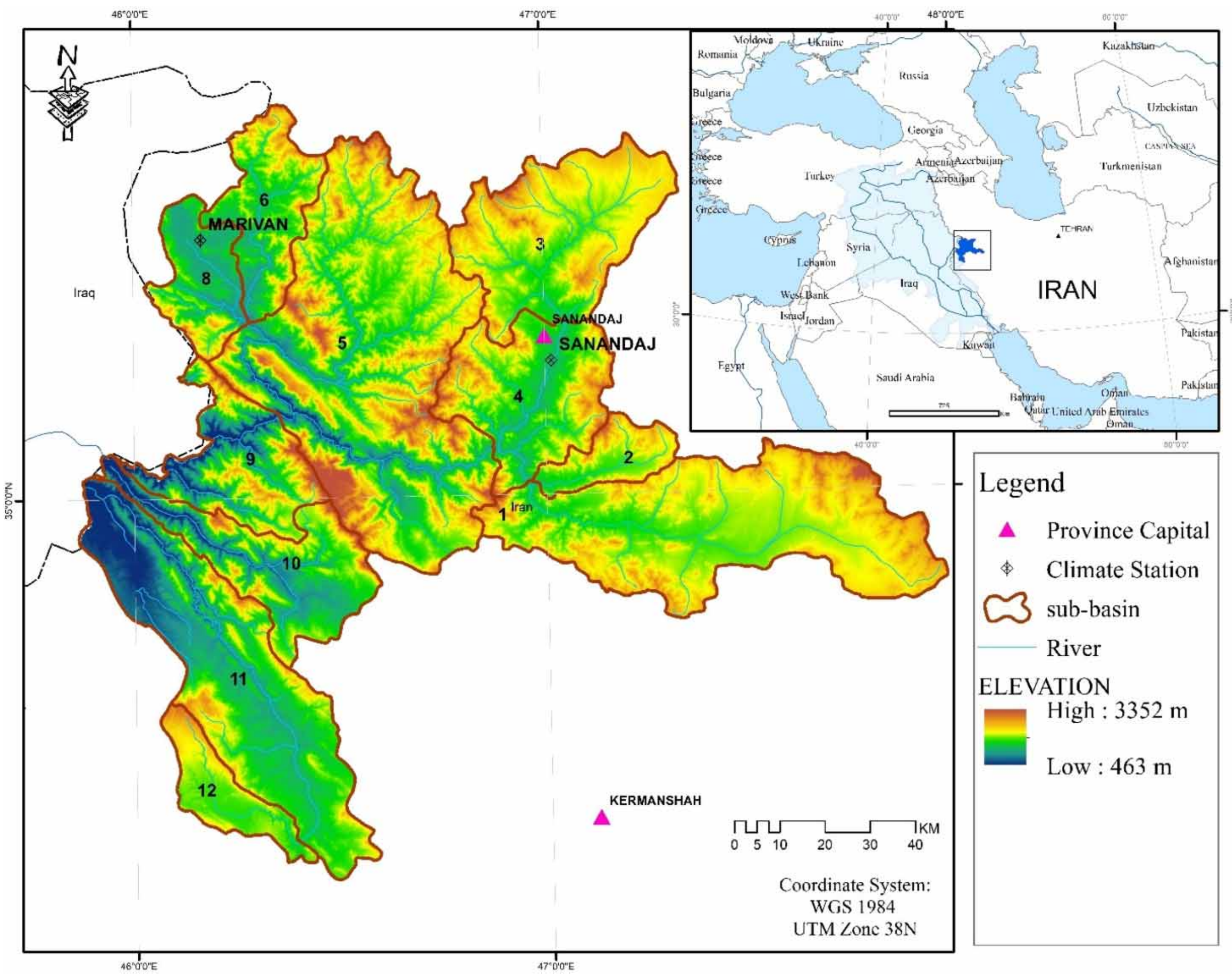

Figure 1 | The location of the study area.

Table 1 | The characteristics of climate stations

	Established year	Longitude	Latitude	Elevation (m)	Station type	Min temperature	Max temperature	Mean temperature	Min precipitation	Max precipitation	Mean precipitation
Marivan Climate station	1991	46° 12′	35° 31′	1,286	Synoptic	5.4°	21.4°	13.4°	452 mm	1,307 mm	894 mm
Sanandaj climate station	1959	47° 80′	35° 20′	1,373	Synoptic	5.8°	21.9°	13.8°	232 mm	794 mm	330 mm

Reference: www.irimo.ir.

Table 2 | The data used and their characteristics

	type	Data	unit	resolution	date	source	tool
Land use	Spatial-temporal	Land use 2019 Land sat 8-OLI	meter	30*30	2019 July	USGS.gov	ENVI5.3 Arc GIS 10.7
Climate	Climatology and synoptic data	Reference evapotranspiration	mm		2019	National meteorological Organization + World climate data	
		Precipitation	mm				
Land data	Spatial	Root restricting layer depth	mm	30*30	2019	Harmonized world soil data FAO.org 1998	Arc GIS 10.7 InVEST 3.8.9
		Plant Available Water Content	–				
		Land use/land cover	–			Processed satellite image	
		Watersheds	–			National Cartographic Center	
		Subbasins	–				
	Table format data	lucode	–		2019		Excel 2019
		LULC_desc	–				
		LULC_veg	–				
		root_depth	mm				
		Kc	–	FAO.org			

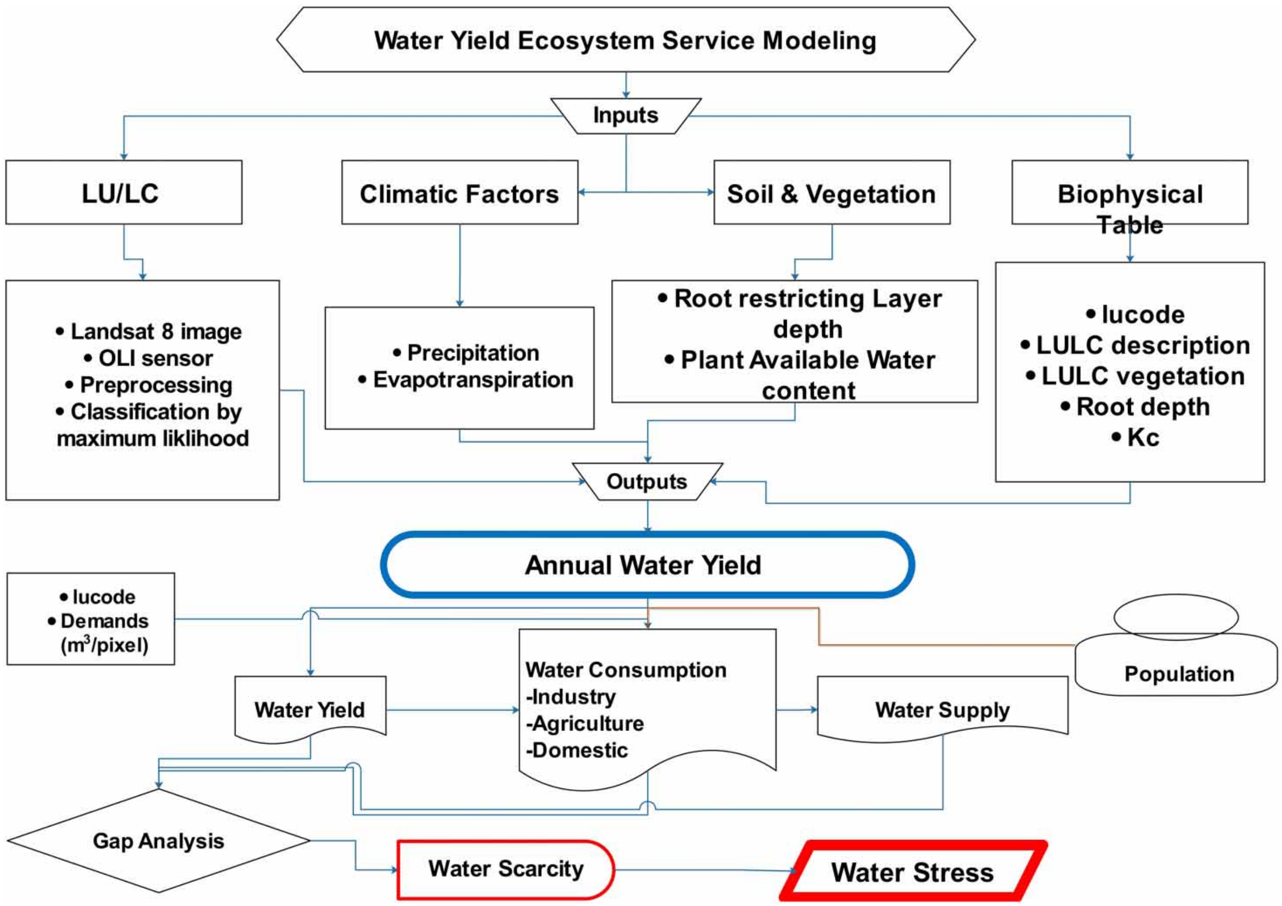

Figure 2 | The conceptual model of the study (authors).

MODEL INPUTS AND PARAMETRIZATION

Preparation of land use map

Land use map was prepared using satellite images (Table 1). To this end, the image of July 2019 was selected from the OLI (Operational Land Imager) sensor of the Landsat 8 satellite. Next, after performing radiometric and atmospheric corrections and ground reference (Ye & Grimm 2013), the image was classified using a maximum likelihood algorithm (Lu & Weng 2007; Hurd & Civco 2009; Shrestha *et al.* 2019).

Image validation is based on ground truth data. For this purpose, 280 points were collected on the ground and then adapted to the generated land use map.

Precipitation

The precipitation parameter in this model is the average annual precipitation map that was prepared using the precipitation map of the world climate data center and downscaling by LARS-WG model using the data of two selected (Sanandaj and Marivan) stations.

Evaporation and transpiration

The evapotranspiration parameter in this model is the map of the average annual evapotranspiration. These data were obtained from the Consultative Group on International Agricultural Research (CGIAR) monthly and then corrected based on the data of two selected stations by downscaling by LARS-WG model and prepared as an annual map.

Root restricting layer depth

The parameter in this model is in the form of a raster map in millimeters, showing the depth of soil that the roots of plants and trees can penetrate. The International Soil Reference and Information Center (ISRIC) data were used to prepare this layer, the accuracy of which was measured by examining the vegetation and trees of the area.

Plant available water content

The parameter plant available water content in the model, which is a fraction of 1, is presented as a map showing the amount of water in the soil that plants can use. The map is based on the soil texture map, soil depth, soil porosity, prepared using ISRIC data and the National Soil and Water Research Center data. Table 3 shows the general characteristics of the main soil texture of the region. This information was prepared in SPAW software 6.02.74 (Table 3).

Population

Increasing population density becomes a significant pressure for sustainable development. It is necessary to manage population pressure according to the ecosystem's capacity to absorb the demand in an optimally sustainable way (Rajput & Sinha 2020). The population parameter is determined based on political boundaries (province, city, and district). The district unit was the most consistent unit on the boundaries of sub-basins by examining the country divisions to calculate the population at the basin level and sub-basins. Thus, the population of each sub-basin was determined by extracting the population of the districts and matching it with the sub-basins. Then, the population density is estimated by dividing the number of people in the area (n/ha).

Modeling water yield, demand, scarcity, and stress

The water yield model was modeled in the InVEST 3.8.9 software. The model was used to evaluate water yield in different studies around the world (Eastman 2015; Hamel & Guswa 2015; Pessacg *et al.* 2015; Jafarzadeh *et al.* 2019; Yang *et al.* 2019; Hu *et al.* 2020; Rahimi *et al.* 2020). The model is based on the Budyko curve (Budyko 1974) and annual precipitation. Also, it

Table 3 | Hydrological characteristics of the region soil

Soil texture	Wilting point (% vol)	Field capacity (% vol)	Saturation (% vol)	Available water (mm/m)	Sat. hydraulic cond. (mm/hr.)	Matric bulk density (kg/m^3)
Clay	29.7	42.2	49.3	118	0.762	1,342
Loam	11.4	24.8	42.9	126	14.73	1,513
Clay loam	20.4	34.3	45.6	130	3.55	1,441

is a practical approach for estimating ecosystem services like water at various scales (Yin *et al.* 2020). In this model, first, the average annual water yield per pixel (Y (x)) of the region is calculated according to Equation (1) (Sharp *et al.* 2019).

$$Y(x) = \left(1 - \frac{AET(x)}{P(x)}\right) \cdot P(x) \quad (1)$$

where AET (x) is the average annual actual evapotranspiration of cell x, and P (x) is the average annual precipitation of the same cell.

In the InVEST water yield model, the land-use layer is divided into two classes with vegetation and no vegetation, and the ratio $AET(x)/P(x)$ of each class is calculated separately. For the covered class, this ratio is calculated based on the Budyko curves proposed by Fu (1981) and Zhang *et al.* (2004) (Equation (2)).

$$\frac{AET(x)}{P(x)} = 1 + \frac{PET(x)}{P(x)} - \left[1 + \left(\frac{PET(x)}{P(x)}\right)^{w}\right]^{\frac{1}{w}} \quad (2)$$

PET (x) is the potential annual evapotranspiration of cell x and w (x) is a non-physical parameter that depends on the natural climatic-soil characteristics of the cell. Potential evapotranspiration, PET (x), is defined according to Equation (3):

$$PET(x) = K_c(L_x) \cdot ET_0(x) \quad (3)$$

where ET0 (x) is a parameter reflecting the climatic conditions of the region based on the evapotranspiration of a reference plant in the region and Kc (Lx) is mainly determined by the vegetation characteristics of the cell soil (Allen *et al.* 1998).

W (x) is an experimental parameter that can be measured by a linear equation $AWC*N/P$, where N is the number of precipitation events per year and AWC is plant available water content (mm). This linear equation is like Equation (4) (Donohue *et al.* 2012):

$$w(x) = Z\frac{AWC(x)}{P(x)} + 1.25 \quad (4)$$

where AWC (x) is plant available water content (mm) in cell x, depending on the soil texture and the adequate root depth. AWC (x), which specifies the amount of water that the soil retains for plant use, is obtained by multiplying the plant available water content capacity (PAWC) at the root restricting depth or plant root depth given in Equation (5) (Yang *et al.* 2019):

$$AWC(x) = Min(Rest \cdot layer \cdot depth, root \cdot depth) \cdot PAWC \quad (5)$$

Root restricting layer depth is the depth that the root cannot penetrate the soil due to the physicochemical properties of the soil. Plant root depth is usually considered the depth at which 95% of the root biomass is present. PAWC is the difference between soil water holding capacity and plant wilting point (Yang *et al.* 2019).

The hydrological parameter Z is an experimental constant between 1 and 30 that shows the local precipitation pattern, precipitation intensity, seasonal climate change, and the topographic characteristics of the basin. The Z parameter calculated use Equation N * 0.2, where N is the number of rainy days per year (Donohue *et al.* 2012).

For the classes without vegetation of the land use layer (like urban areas and wetlands), the actual evapotranspiration of AET (x) is obtained directly from the evapotranspiration of the reference ET0 (x) according to Equation (6):

$$AET(x) = Min(K_c(L_x).ET_0(x), P(x)) \quad (6)$$

where ET0 (x) is the reference evapotranspiration and Kc (Lx) the specific land use evaporation factor (Table 4).

The relative index of water scarcity and stress

This index is calculated using the ratio of water consumption in each sub-basin based on agricultural and residential lands and population. Then, it is evaluated based on the thresholds of Table 5 (Equation (7)). The index was developed by Vörösmarty

Table 4 | Land use and its evapotranspiration coefficient

Row	Land use	Lu-code	k_c	Root depth (mm)	Vegetation	LU/LC (%)	Water demand (m^3/yr./pixel)
1	Built-up	1	0.7	0	0	1.44	400
2	Water	2	1	0	0	0.44	0
3	Forest	3	0.95	2,000	1	13.07	0
4	Agriculture	4	0.9	1,000	1	15.15	200
5	Rangeland	5	0.8	300	1	52.52	0
6	Dry farming	6	0.4	200	1	14.13	0
7	Bare land	7	0.5	0	0	2.25	0
Source	Author	Author	FAO 1998	ISRIC	Author	Author	Estimated based on national per capita consumption data

Table 5 | Thresholds of water scarcity and stress

Category	Contemporary WSI threshold (m^3 $capita^{-1}year^{-1}$)
No stress	1,700<
Water scarcity	1,000–1,700
Water stress	500–1,000
Absolute water stress	500>

Damkjaer & Taylor (2017).

et al. (2000) and in 2009 by Vörösmarty and the Department of Water Systems Analysis, the University of New Hampshire in the Second World Water Development Report (Vörösmarty *et al.* 2000; Vörösmarty *et al.* 2005; WSAG 2009).

$$RWSI = DIA/Q \tag{7}$$

Here, RWSI is the relative index of water stress, 'D' is domestic water consumption, 'I' is industrial water consumption, 'A' is agricultural water consumption, and 'Q' is the water supplied at the basin level. According to this index, the water stress boundary is denoted by a threshold of 0.4.

The thresholds for this and other water stress indices were examined by Damkjaer & Taylor (2017). According to these authors, many scholars mistakenly equate the water scarcity index with the water stress index. According to Table 5, water scarcity and stress index is based on their studies (Damkjaer & Taylor 2017). Hence, the thresholds are calculated based on the index of Formula 7, Table 5, and Figure 3 in the study.

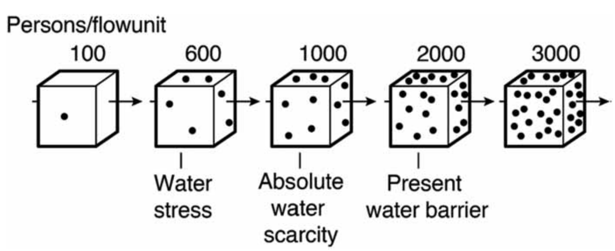

Figure 3 | Visualization of different levels of water competition; each cube indicates the flow of 1 million m^3/year available in terrestrial water systems, each dot 100 individuals depending on that water *(Adapted from Falkenmark 1989, p. 115.*

RESULTS

Land use

Figure 4 presents the land use map of the area. The map has 7 classes including built-up areas (1.44%) like cities, villages, airports and industries, water bodies (0.44%) including lakes and dams, forests (13.07%), agriculture (15.15%) including irrigated agricultural lands, rangeland (52.52%), dry farming (15.13%), and barren lands (2.25%) including areas without vegetation (Figure 3). To evaluate the classification accuracy, we collected 280 ground points and compared them with the classified image. The results showed that 94% of the points are correct. Most land uses of the region are rangelands, agricultural, forest, and dry farming. More forests are in the western half of the basin and dry farming is more in the eastern half. Due to the region's climate and soil conditions, barren lands in this region are very limited, although they increase due to excessive human use, especially overgrazing.

Root depth

Figure 5(a) shows the root restricting depth map to which the roots can penetrate because of the physicochemical properties of the soil. Considering the depth of soil in the area examined, in the eastern regions, with a lower slope and more plains, and older in age than the western regions, the soil depth is greater. Also, the soil texture is more developed in these regions, and

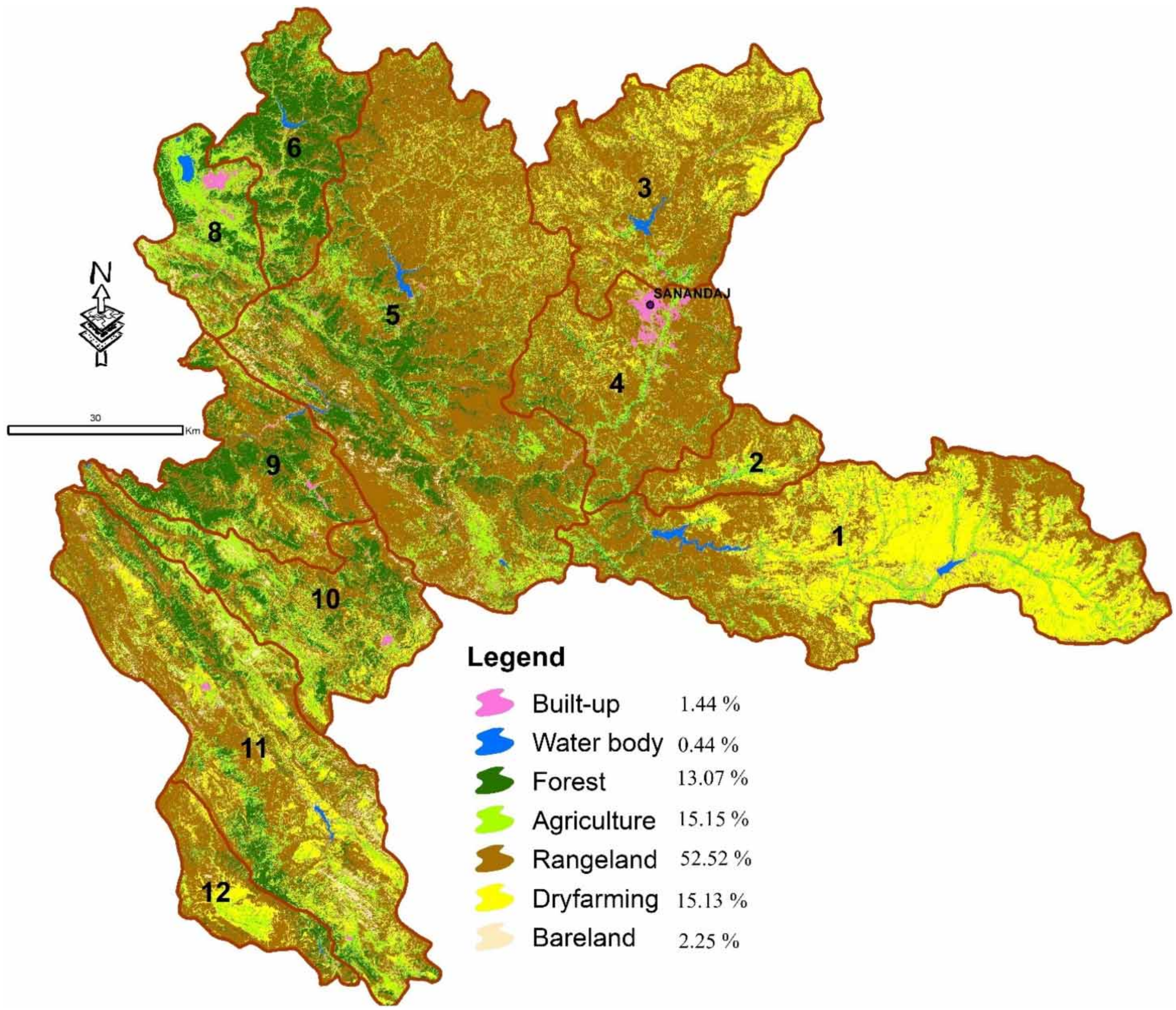

Figure 4 | The land use of the region.

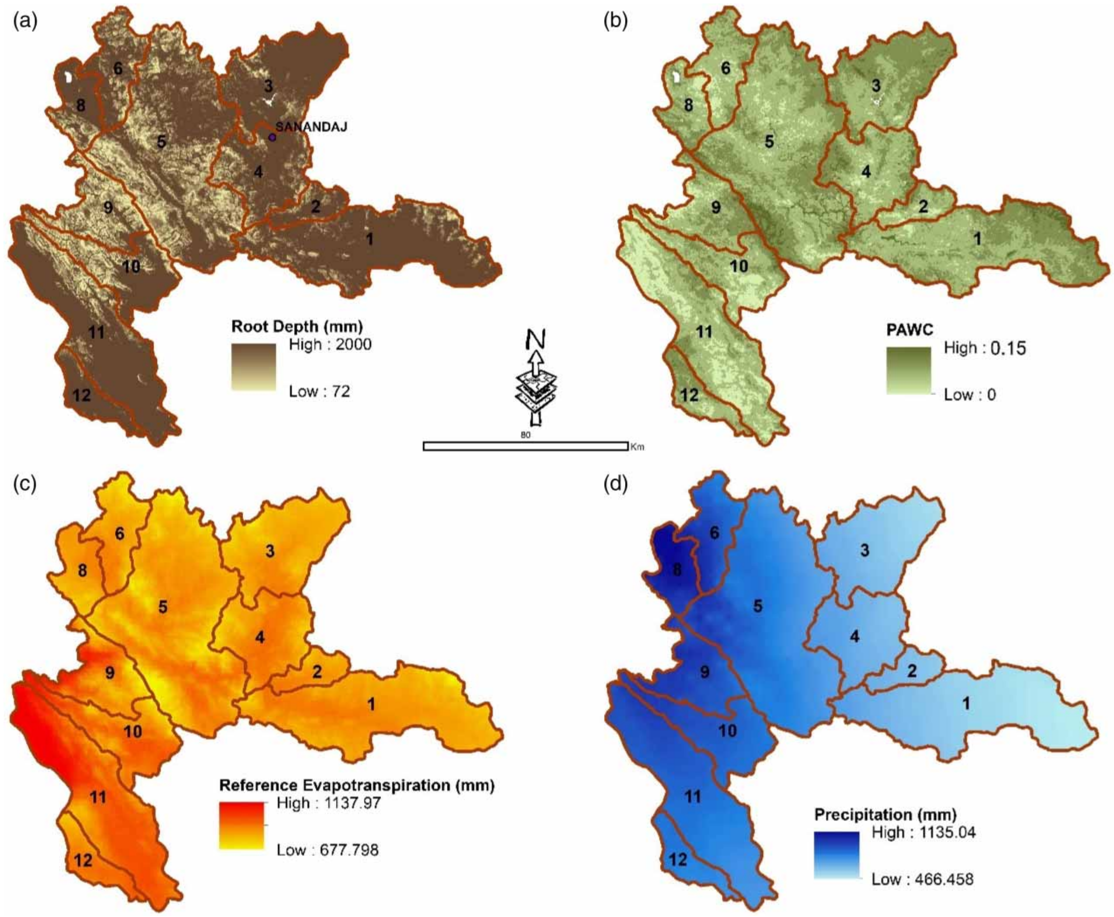

Figure 5 | Root restricting layer depth (a), plant available water content (b), evapotranspiration (c), and precipitation map (d) across sub-basins of the study area.

thus the water-retaining capacity is higher. Based on the land use map of the study area, agricultural lands are more expanded and are exploited in dry farming and irrigating forms.

Plant available water content

Figure 5(b) presents the plant's available water content. This parameter indicates the amount of water stored in the soil that is available for plant use. A part of the water from precipitation is retained after penetrating the soil layer, and another part is used by plants through plant roots if there is vegetation. This amount of water is called plant available water content (Veihmeyer and Hendrickson 1931). In this model, this content is expressed as a fraction of 1. The maximum value of this parameter in the region is 0.15, indicating that the plant can consume 15% of the water in the soil.

Evapotranspiration

Figure 5(c) shows the annual reference evapotranspiration parameter with a minimum of 677 mm and a maximum of 1,137 mm. This parameter plays a pivotal role in determining water yield as it causes the loss of a large part of precipitation. The highest evapotranspiration rate has occurred at the basin outlet, probably due to the high temperature in this area.

Precipitation

In Figure 5(d), the precipitation map is shown in the raster (cell-based) format. Precipitation in the study area declines from west to east, with the lowest precipitation being 466 mm in the easternmost point of the region and the highest precipitation in the west of the region 1,135 mm. Precipitation has a critical role as the main factor of water yield in any region.

Water yield, consumption, scarcity and stress

Figure 6(a) shows water yield in cubic meters at the surface of each sub-basin. Sub-basins 5, 11, and 1 have the highest water yield volume. This high volume in this sub-basin, in addition to the average precipitation, evaporation, soil and land use characteristics, is also due to their area.

To model validation, its results were compared with each sub-basin's actual water yield statistics in Table 6. There is a high correlation between the model results and the real statistics.

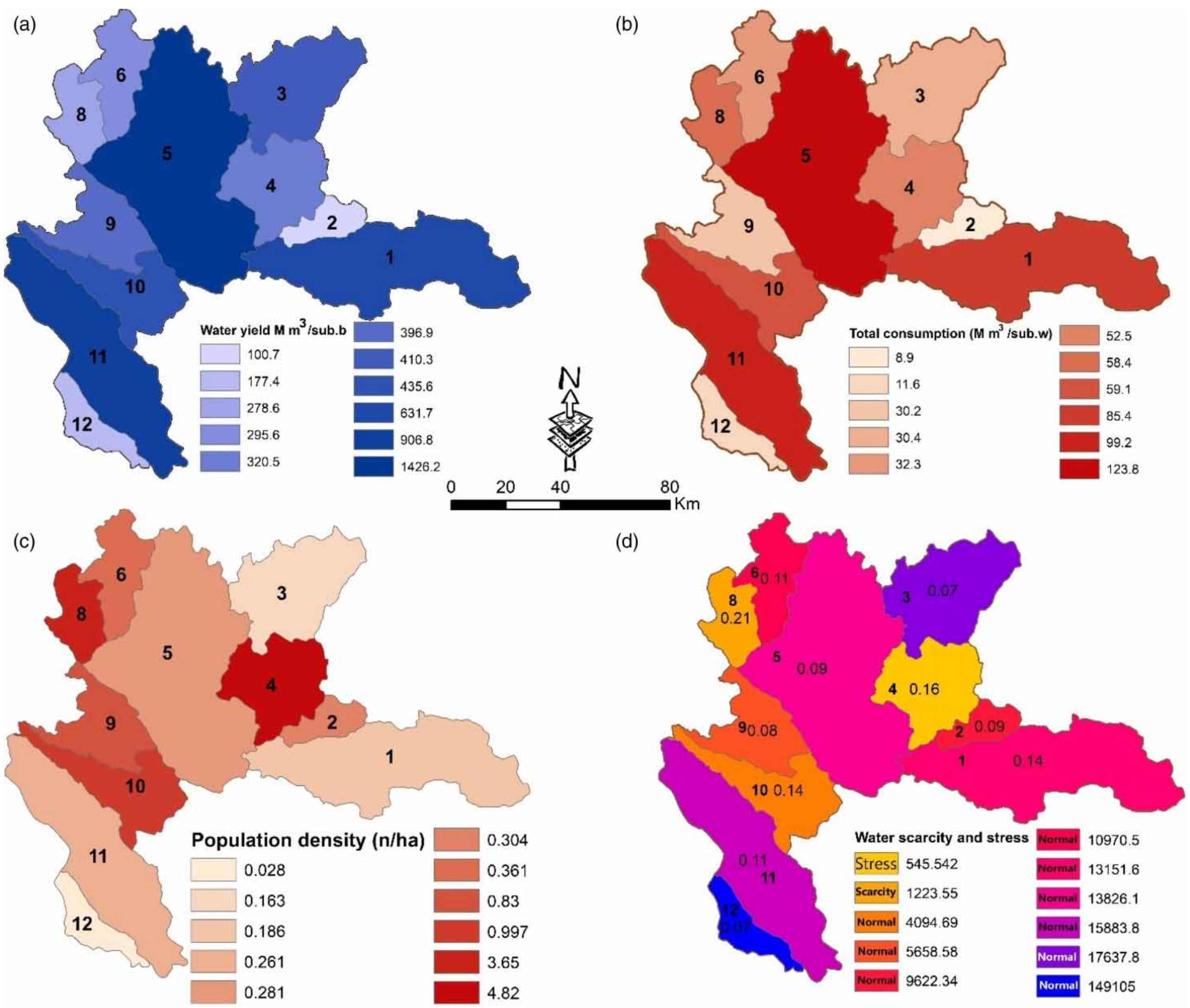

Figure 6 | Maps of water yield (a), water consumption (b), population density (c), and water scarcity and stress index (d) across sub-basins of the study area.

Table 6 | Model validation

Sub-basin number	1	2	3	4	5	6	8	9	10	11	12	Total
Model results (M.m^3/yr)	733		731		1,722		279	397	436	1,084		5,382
National statistics (M.m^3/yr)	724		593		1,802		264	395	404	925		5,107
Different (%)	1.24		23		−4.43		5.68	0.5	7.92	17.18		5.38

Water consumption (Figure 6(b)) is directly derived from the water needed for agricultural and construction uses, calculated according to the per capita domestic, industrial and agricultural uses in the region. Per capita domestic, industrial, and agricultural consumption is 85, 40, and 485 cubic meters per year, respectively (water resource management of Kurdistan province 2019). In estimating the volume of consumption and calculating the per capita triple consumption, the area of built-up and agriculture land use of each sub-basin was also used.

Figure 6(c) presents the population density map of the study area. The population density in sub-basins 4, 8, and 10 is higher than in other areas. On the other hand, sub-basins 12, 2, 3, and 6 have the lowest population density.

Figure 6(d) illustrates water scarcity and stress indices. The result of the index is shown in two ways. Firstly, Table 5 shows the state of water scarcity and stress. Accordingly, sub-basins 8 and 4 experience water scarcity and water stress, respectively. Moreover, according to Equation (8), whose result is plotted on the map, sub-basins 2 and 4 are in a state of instability but they have not yet reached water stress.

DISCUSSION

Water resource modeling aims to provide insightful information and use it in planning to use this resource (Loucks & Beek 2017). The present study modeled water resources according to ecosystem services and evaluated their situation in the region based on water scarcity and stress index. According to the results, water yield is affected by various parameters. Land use as one of the parameters has a vital role in water yield.

In the Sirvan river basin, rangelands are the most considerable land use covering 52% of the area. Forest land uses exist mostly in the western half, while the dry farming land uses are more in the eastern half. Built-up land use is more affected by the three urban areas. This important parameter must be updated regularly regarding its role in modeling. In this process, satellite images are a good source for preparing the land use map. Besides, the Landsat satellite and OLI sensor are suitable for mid-scale studies like this due to their availability and quality (Ghayour *et al.* 2021). The classification method is essential in image accuracy, as well. In the study, the maximum likelihood classification method (Mohajane *et al.* 2018) was used with an accuracy of 94%.

Climatic parameters play a pivotal role in water yield. Since precipitation in this region does not have a similar distribution and decreases from west to east, evapotranspiration is higher in the southwestern regions, where the basin's outlet is, than the other areas. The accuracy of the climatic data used in the study is acceptable given that it is the result of global, local, and modeling data. Daily data from two stations in Sanandaj in the east and Marivan in the west of the basin were used for downscaling with the LARS-WG model. Data from these two stations also were used to evaluate the accuracy of the model and global data. The precipitation difference in the west of the region is due to the Zagros Mountains, which block the western air masses making these clouds fall (Kiani & Abolfathei 2021).

The soil parameter is assumed to have a fundamental role in water yield from the surface of a basin based on its characteristics. Depending on their depth and texture, soils can be penetrated by water or prevent its penetration. Additionally, they can limit the penetration of plant roots. Hence, using the soil depth layer and the water stored in it is necessary for modeling water resources (Jafarzadeh *et al.* 2019). In sub-basins 1, 3, 8, 11, and 12, soil depth is more than other areas. This depth is affected by the region's topography and slope. In these sub-basins, the mountains are as substantial hills.

Meanwhile, there are higher altitudes and slopes in the sub-basins where the soil depth is shallow. Agricultural lands with steep slopes have higher volumetric density and lower infiltration rate, while forest slopes with gentle slopes have lower volumetric densities and higher permeability (Wubie & Assen 2020). Thus, water yield in agricultural lands and steep slopes can be more than that in forestlands and gentle slopes.

As already stated, water yield is affected by land use, precipitation, evapotranspiration, and soil characteristics (Sadeghi *et al.* 2021; Soomro *et al.* 2021). Sub-basins 5, 11, and 1 have the highest water yield volume, while sub-basins 2, 12, and 8 have the lowest water yield. In addition to the parameters mentioned, the production volume affects the area of each sub-basin as well. According to the obtained results, the average water yield per unit area in the western regions is higher because of the high precipitation. However, as this water accumulates on the surface of the basins, flows, and is calculated as runoff, it has a higher volume in larger basins. Water consumption is a critical parameter that needs proper planning according to the production value so that the situation of this important source is not disrupted in supply and imbalanced. Water consumption is a function of the population and its water needs (Tholiya *et al.* 2021). Population density increasing caused increasing water demand in respect of different types of usage. The demand for more food production, more power generation, and more industrial expansion for economic development is directly or indirectly correlated with the increase in population pressure (Rajput & Sinha 2020). The largest populations are in sub-basins 4 and 8, yet the consumption volume is highest in sub-basins 5, 11, and 1. Considering the per capita agriculture, which is somehow 6 times the per capita domestic consumption, and the agricultural land areas in sub-basins 5, 11, and 1, and the area of these sub-basins, their consumption rate is greater compared to that of other sub-basins. In addition to population size, its distribution is critical in resource planning and can disrupt water supply. In recent decades, population growth in this area has increased rapidly, and the rate of urbanization has increased such that about 70% of the population living in this basin lives in urban areas. Moreover, the urban areas in this basin are often located in small sub-basins, which is a factor in the imbalance of supply and demand.

Population and its needs are the main driving forces in demand for land, water, and energy (Imasiku & Ntagwirumugara 2020). Eighty people per square kilometer are living in the Sirvan river basin. According to official statistics, the per capita consumption of agriculture, household, and industry is 610 cubic meters per year, and according to the thresholds introduced by Falkenmark & Lindh (1976), Vörösmarty, *et al.* (2005), and Damkjaer & Taylor (2017), less than 500 m^3/yr shows absolute water stress, less than 1,000 m^3/yr indicates water stress, 1,700 m^3/yr shows water scarcity, and more than 1,700 m^3/yr indicates no stress and scarcity. In this basin, out of the total per capita of 610 cubic meters per year, the share of domestic water use is 13.5%, industrial water 6.5%, and agricultural water 80%. The current average per capita consumption in this basin is 61% of the threshold of 1,000 meters. Therefore, low per capita consumption is considered as a water scarcity threshold (1,000) in this basin due to the semi-arid region, dry farming, and the lack of large industries. The semi-arid region is affecting in two ways: because of the considerable precipitation and mountainous and cold climate and humidity regime, there is the possibility of dry farming, reducing the per capita water consumption in agriculture. On the other hand, the semi-arid region and limited resources cause adaptation to the existing conditions and decrease per capita compared to the declared threshold (1,000).

Water resources planning and management, especially in arid areas, has always been a significant challenge. In recent decades, with the growth of the human population, the demand for this resource has constantly been increasing. On the other hand, factors like climatic change have affected the supply of this resource, complicating the situation and leading to a more considerable planning challenge. Understanding the status quo is very important in planning. As many parameters are involved in understanding the status quo, efforts are made to reach more accurate models and approaches. Proper use of these parameters is critical as they determine reaching the right results. Some of the existing methods and models allow users to know the current situation spatially or geographically. These models include SWAT (Akoko *et al.* 2020; Brouziyne *et al.* 2020; Petpongpan *et al.* 2020; Li *et al.* 2021; Wang & Cao 2021), WEAP (Li *et al.* 2015; Gao *et al.* 2017), and InVEST model (Yang *et al.* 2020; Yin *et al.* 2020), all having both capabilities and limitations. The accuracy of the inputs of each model is a critical feature. Overall, modeling water resources according to the concept of ecosystem services is a new approach to identify the available source and highlight the significance of ecosystems and work to preserve them, which is carried out using the InVEST model.

CONCLUSION

Water resources planning is critical to meet the sustainable needs of humans and the sustainability of ecosystems considering the increase in population and climate change in semi-arid regions. According to the concept of ecosystem services, modeling water supply and demand and the sustainability of provision of this resource can be effective in protecting ecosystems. Population growth and its displacement can hamper the sustainable supply of ecosystem services (water). As the population grows, the demand for water, agricultural land, and residential land increases, disrupting the resource supply process and destroying the ecosystem. These changes lead to water scarcity and stress at the surface of basins and sub-basins. Modeling with InVEST presents valuable information for water resource planners according to land use and climatic parameters. The modeling results showed that 5,381 million m^3 of water is produced per year in the Sirvan river basin with 11 sub-basins. Considering the type of land uses, the area of each sub-basin, the resident population in each sub-basin, precipitation, and evapotranspiration, water scarcity and stress were identified in sub-basins 4 and 8. Scarcity and stresses in the resources needed, especially water, can lead to various environmental and social problems because it is directly associated with food security and public health.

Moreover, by disregarding the environmental water requirements of ecosystems, its destructive effects will ultimately affect human society. Hence, modeling based on ecosystem services and accurate and useful data can be planned for existing resources. For more accurate planning, it is recommended to perform this modeling for future periods and reduce tensions, population policies, and development using climate data and land-use change.

DATA AVAILABILITY STATEMENT

Data cannot be made publicly available; readers should contact the corresponding author for details.

REFERENCES

Akoko, G., Kato, T. & Tu, L. H. 2020 Evaluation of irrigation water resources availability and climate change impacts – a case study of Mwea Irrigation Scheme, Kenya. *Water* **12**, 1–22.

Allen, R. G., Pereira, L. S., Raes, D. & Smith, M. 1998 *Crop evapotranspiration-Guidelines for computing crop water requirements-FAO Irrigation and Drainage*, paper 56. FAO, Rome 300.

Balist, J., Malekmohammadi, B., Jafari, H. R., Nohegar, A. & Geneletti, D. 2022 Detecting land use and climate impacts on water yield ecosystem service in arid and semi-arid areas. A study in Sirvan River Basin-Iran. *Applied Water Science* **12**, 4. https://doi.org/10.1007/s13201-021-01545-8.

Baloch, M. A., Ames, D. P. & Tanik, A. 2015 Hydrologic impacts of climate and land-use change on Namnam Stream in Koycegiz Watershed, Turkey. *International Journal of Environmental Science and Technology* **12** (5), 1481–1494.

Bonan, G. 2015 *Ecological Climatology: Concepts and Applications*. Cambridge University Press, Cambridge, UK.

Bouguerra, S. & Jebari, S. 2017 Identification and prioritization of sub-watersheds for land and water management using InVEST SDR model: Rmelriver basin, Tunisia. *Arabian Journal of Geosciences* **10**, 348.

Brauman, K. A. 2015 Hydrologic ecosystem services: linking ecohydrological processes to human well-being in water research and watershed management. *Water* **2**, 345–358.

Brouziyne, Y., Abouabdillah, A., Chehbouni, A., Hanich, L., Bergaoui, K., McDonnell, R. & Benaabidate, L. 2020 Assessing hydrological vulnerability to future droughts in a Mediterranean watershed: combined indices-based and distributed modeling approaches. *Water* **12**, 2333.

Budyko, M. I. 1974 *Climate and Life*. Academic Press, New York, NY.

Cabral, P., Campos, F. S., David, J. & Caser, U. 2021 Disentangling ecosystem services perception by stakeholders: an integrative assessment based on land cover. *Ecological Indicators* **126**, 107660.

Chacko, S., Kurian, J., Ravichandran, C., Vairavel, S. M. & Kumar, K. 2019 An assessment of water yield ecosystem services in Periyar Tiger Reserve, Southern Western Ghats of India. *Geology, Ecology, and Landscapes* **5** (1), 32–39.

Chen, Y., Wang, K., Lin, Y., Shi, W., Song, Y. & He, X. 2015 Balancing Green and grain trade. *Nature Geoscience* **8**, 739–741.

Costanza, R., de Groot, R., Sutton, P., van der Ploeg, S., Anderson, S. J., Kubiszewski, I., Farber, S. & Kerry Turner, R. 2014 Changes in the global value of ecosystem services. *Global Environmental Change* **26**, 152–158.

Damkjaer, S. & Taylor, R. 2017 The measurement of water scarcity: defining a meaningful indicator. *Ambio* **46** (5), 513–531.

Donohue, R. J., Roderick, M. L. & McVicar, T. R. 2012 Roots, storms and soil pores: incorporating key ecohydrological processes into Budyko's hydrological model. *Journal of Hydrology* **436**, 35–50.

Eastman, J. R. 2015 TerrSet. Guide to GIS and image processing. Clark University, Worcester, MA.

Falkenmark, M. & Lindh, G. 1976 Water for a starving world. Westview Press, Boulder, CO.

FAO 1998 Crop evapotranspiration – guidelines for computing crop water requirements – FAO Irrigation and drainage paper 56. Available from: http://www.fao.org/3/x0490e/x0490e00.htm#Contents.

Fu, B. P. 1981 On the calculation of the evaporation from land surface. *Atmospheric Sciences* **5**, 23–31. (in Chinese).

Gao, J., Christensen, P. & Li, W. 2017 Application of the WEAP model in strategic environmental assessment: experiences from a case study in an arid/semi-arid area in China. *Journal of Environmental Management* **198** (1), 363–371.

Ghayour, L., Neshat, A., Paryani, S., Shahabi, H., Shirzadi, A., Chen, W., Al-Ansari, N., Geertsema, M., Pourmehdi Amiri, M., Gholamnia, M., Dou, J. & Ahmad, A. 2021 Performance evaluation of Sentinel-2 and Landsat 8 OLI data for land cover/use classification using a comparison between machine learning algorithms. *Remote Sensing* **13**, 1349.

Gheewala, S. H., Silalertusksa, T., Nilsalab, P., Mungkung, R., Perret, S. R. & Chaiyawannakarn, N. 2014 Water footprint and impact of water consumption for food, feed, fuel crops production in Thailand. *Water* **6**, 1698–1718.

Gheewala, S. H., Silalertruksa, T., Nilsalab, P., Lecksiwilai, N., Sawaengsak, W., Mungkung, R. & Ganasut, J. 2018 Water stress index and its implication for agricultural land-use policy in Thailand. *International Journal of Environmental Science and Technology* **15**, 833–846.

Grizzetti, B., Lanzanova, D., Liquete, C., Reynaud, A. & Cardoso, A. C. 2016 Assessing water ecosystem services for water resource management. *Environmental Science & Policy* **61**, 194–203.

Haiping, L., Yanan, Q. & Yunying, Q. 2018 Use a spatial analysis model to assess habitat quality in Lashihai watershed. *Journal of Resources and Ecology* **9** (6), 622–631.

Hamel, P. & Guswa, A. J. 2015 Uncertainty analysis of a spatially explicit annual water-balance model: case study of the Cape Fear basin, North Carolina. *Hydrology and Earth System Sciences* **19** (2), 839–853.

He, S. & Wu, J. 2019 Relationships of groundwater quality and associated health risks with land use/land cover patterns: a case study in a loess area, northwest China. *Hum Ecol Risk Assess* **25** (2), 354–373. http://doi.org/10.1080/10807 039.2019.15704 63.

He, X., Estes, L., Konar, M., Tian, D., Anghileri, D., Baylis, K., Evans, T. P. & Sheffield, J. 2019 Integrated approaches to understanding and reducing drought impact on food security across scales. *Curr Opin Environ Sustainability* **40**, 43–54. Available from: https://data.irimo.ir.

Hu, W., Li, G., Gao, Z., Jia, G., Wang, Z. & Li, Y. 2020 Assessment of the impact of the Poplar Ecological Retreat Project on water conservation in the Dongting Lake wetland region using the InVEST model. *Science of the Total Environment* **733**, 139423.

Hurd, J. D. & Civco, D. L. 2009 Creating an image dataset to meet your classification needs: A proof-of-concept study. In *Proceedings of the ASPRS Annual Conference*, Baltimore, MD, USA, pp. 9–13.

Imasiku, K. & Ntagwirumugara, E. 2020 An impact analysis of population growth on energy-water-food-land nexus for ecological sustainable development in Rwanda. *Food and Energy Security* **9**, 185.

Jafarzadeh, A., Mahdavi, A., FallahShamsi, R. & Yousefpour, R. 2019 Annual water yield estimation for different land uses by GIS-Based InVEST model (Case study: Mish-khas Catchment, Ilam Province, Iran). *Journal of Rangeland Science* **9** (1), 1–12.

Kiani, M. & Abolfathei, D. 2021 The precipitation changes on the western and eastern aspects of Zagros mountains. *Journal of Environmental Sciences Studies* **6** (1), 3494–3498.

Lang, Y., Song, W. & Deng, X. 2017 Projected land-use changes impacts on water yields in the karst mountain areas of China. *Physics and Chemistry of the Earth* **11**, 001.

Li, X., Zhao, Y., Shi, C., Sha, J., Wang, Z.-L. & Wang, Y. 2015 Application of Water Evaluation and Planning (WEAP) model for water resources management strategy estimation in coastal Binhai New Area, China. *Ocean & Coastal Management* **106**, 97–109.

Li, Y., Piao, S., Li, L. Z. X., Chen, A., Wang, X., Ciais, P., Huang, L., Lian, X., Peng, S., Zeng, Z., Wang, K. & Zhou, L. 2018 Divergent hydrological response to large-scale afforestation and vegetation greening in China. *Science Advances* **4**, 4182.

Liu, J., Yang, H., Gosling, S. N., Kummu, M., Flörke, M., Pfister, S., Hanasaki, N., Wada, Y., Zhang, X., Zheng, C., Alcamo, J. & Oki, T. 2017 Water scarcity assessments in the past, present, and future. *Earth's Future* **5**, 545–559. https://doi.org/10.1002/2016EF000518.

Loucks, D. P. & van Beek, E. 2017 Water resource systems modeling: its role in planning and management. In: *Water Resource Systems Planning and Management*. Springer, Cham. https://doi.org/10.1007/978-3-319-44234-1_2.

Lu, D. & Weng, Q. 2007 A survey of image classification methods and techniques for improving classification performance. *International Journal of Remote Sensing* **28**, 823–870.

Mohajane, M., Essahlaoui, A., Oudija, F., Hafyani, M. E., Hmaidi, A. E., Ouali, A. E., Randazzo, G. & Teodoro, A. C. 2018 Land Use/Land Cover (LULC) Using Landsat Data Series (MSS, TM, ETM+ and OLI) in Azrou Forest, in the Central Middle Atlas of Morocco. *Environments* **5** (12), 131.

Pessacg, N., Flaherty, S., Brandizi, L., Solman, S. & Pascual, M. 2015 Getting water right: a case study in water yield modelling based on precipitation data. *Science of the Total Environment* **537**, 225–234.

Petpongpan, C., Ekkawatpanit, C. & Kositgittiwong, D. 2020 Climate change impact on surface water and groundwater recharge in Northern Thailand. *Water* **12**, 1029.

Peyman, Y., Avand, M., Abbaspour, R. A., Karami, M. & Tiefenbachere, J. P. 2020 GIS-based spatial modeling of snow avalanches using four novel ensemble models. *Science of The Total Environment* **25**, 141008.

Rahimi, L., Malekmohammadi, B. & Yavari, A. R. 2020 Assessing and modeling the impacts of wetland land cover changes on water provision and habitat quality ecosystem services. *Natural Resources Research* **29**, 3701–3718.

Rajput, P. & Sinha, M. K. 2020 Geospatial evaluation of drought resilience in sub-basins of Mahanadi river in India. *Water Supply* **20** (7), 2826–2844. https://doi.org/10.2166/ws.2020.178.

Redhead, J. W., Stratford, C., Sharps, K., Jones, L., Ziv, G., Clarke, D., Oliver, T. H. & Bullock, J. M. 2016 Empirical validation of the InVEST water yield ecosystem service model at a national scale. *Science of the Total Environment* **1**, 569–570.

Sadeghi, A., Galalizadeh, S., Zehtabian, G. & Khosravi, H. 2021 Assessing the change of groundwater quality compared with land-use change and precipitation rate (Zrebar Lake's Basin). *Applied Water Science* **11**, 170. https://doi.org/10.1007/s13201-021-01508-z.

Sallustio, L., De Toni, A., Strollo, A., Di Febbraro, M., Gissi, E., Casella, L., Geneletti, D., Munafò, M., Vizzarri, M. & Marchetti, M. 2017 Assessing habitat quality in relation to the spatial distribution of protected areas in Italy. *Journal of Environmental Management* **201**, 129–137.

Sharp, R., Tallis, H. T., Ricketts, T., Guerry, A. D., Wood, S. A. & Chaplin-Kramer, R. 2019 *InVEST 3.7.0 Users Guide. The Natural Capital Project*. Stanford University, University of Minnesota, the Nature Conservancy, and World Wildlife Fund.

Shrestha, M., Leigh, L. & Helder, D. 2019 Classification of north Africa for use as an extended pseudo invariant calibration sites (EPICS) for radiometric calibration and stability monitoring of optical satellite sensors. *Remote Sensing* **11**, 875.

Soomro, S.-e-h., Hu, C., Jian, S., Wu, Q., Boota, M. W. & Soomro, M. H. A. A. 2021 Precipitation changes and their relationships with vegetation responses during 1982–2015 in Kunhar River basin, Pakistan. *Water Supply* **21** (7), 3657–3671. https://doi.org/10.2166/ws.2021.129.

Sun, Q., Miao, C., Duan, Q., Ashouri, H., Sorooshian, S. & Hsu, K.-L. 2018 A review of global precipitation data sets: data sources, estimation, and intercomparisons. *Reviews of Geophysics* **56** (1), 79–107.

Tholiya, J. J., Chaudhary, N. & Alam, B. M. 2021 Determinants of geographical inequalities in domestic water supply across city of Pune, India. *Water Supply*. ws2021364. https://doi.org/10.2166/ws.2021.364.

Touch, T., Oeurng, C., Jiang, Y. & Mokhtar, A. 2020 Integrated modeling of water supply and demand under climate change impacts and management options in tributary Basin of Tonle Sap Lake, Cambodia. *Water* **12**, 2462.

Uche, J., Martínez-Gracia, A., Círez, F. & Carmona, U. 2015 Environmental impact of water supply and water use in a Mediterranean water-stressed region. *Journal of Cleaner Production* **88**, 196–204.

Veihmeyer, F. J. & Hendrickson, A. H. 1931 The moisture equivalent as a measure of the field capacity of soils. *Soil Science* **32**, 181–193.

Vörösmarty, C. J., Green, P., Salisbury, J. & Lammers, R. B. 2000 Global water resources: vulnerability from climate change and population growth. *Science* **289**, 284–288.

Vörösmarty, C. J., Douglas, E. M., Green, P. A. & Revenga, C. 2005 Geospatial indicators of emerging water stress: an application to Africa. *Ambio* **34**, 230–236.

Wang, Z. & Cao, J. 2021 Spatial-temporal pattern study on water conservation function using the SWAT model. *Water Supply* **21** (7), 3629–3642. https://doi.org/10.2166/ws.2021.127.

Wang, D., Hubacek, K., Shan, Y., Gerbens-Leenes, W. & Liu, J. 2021a A review of water stress and water footprint accounting. *Water* **13** (2), 201. https://doi.org/10.3390/w13020201.

Wang, Z., Wu, X., Wang, H. & Wu, T. 2021b Prediction and analysis of domestic water consumption based on optimized grey and Markov model. *Water Supply* **21** (7), 3887–3899. https://doi.org/10.2166/ws.2021.146.

Water Systems Analysis Group, University of New Hampshire. Available from: http://www.wsag.unh.edu/ (accessed 3 March 2009). World Resources Institute. Available from: http://www.wri.org (accessed 3 March 2009).

Wubie, M. A. & Assen, M. 2020 Effects of land cover changes and slope gradient on soil quality in the Gumara watershed, Lake Tana basin of North–West Ethiopia. *Modeling Earth Systems and Environment* **6**, 85–97.

Yang, D., Liu, W., Tang, L., Chen, L., Li, X. & Xu, X. 2019 Estimation of water provision service for monsoon catchments of South China: applicability of the InVEST model. *Landscape and Urban Planning* **182**, 133–143.

Yang, X., Chen, R., Meadows, M. E., Ji, G. & Xu, J. 2020 Modelling water yield with the InVEST model in a data scarce region of northwest China. *Water Supply* **20** (3), 1035–1045. https://doi.org/10.2166/ws.2020.026.

Yang, J., Xie, B., Zhang, D. & Tao, W. 2021 Climate and land use change impacts on water yield ecosystem service in the Yellow River Basin, China. *Environmental Earth Sciences* **80**, 72.

Yariyan, P., Avand, M., Abbaspour, R. A., Karami, M. & Tiefenbachere, J. P. 2020 GIS-based spatial modeling of snow avalanches using four novel ensemble models. *Science of the Total Environment* **745** (25), 141008.

Ye, L. & Grimm, N. B. 2013 Modelling potential impacts of climate change on water and nitrate export from a mid-sized, semi-arid watershed in the US Southwest. *Climate Change* **120** (1–2), 419–431.

Yin, G., Wang, X., Zhang, X., Fu, Y., Hao, F. & Hu, Q. 2020 InVEST model-based estimation of water yield in North China and its sensitivities to climate variables. *Water* **12** (6), 1692.

Zhang, L., Hickel, K., Dawes, W. R., Chiew, F. H., Western, A. W. & Briggs, P. R. 2004 A rational function approach for estimating mean annual evapotranspiration. *Water Resources Research* **40** (2), W02502.

Zhang, G. P., Hoekstra, A. Y. & Mathews, R. E. 2013 Water footprint assessment (WFA) for better water governance and sustainable development. *Water Resources and Industry* **1–2**, 1–6.

Zhang, L., Cheng, L., Chiew, F. & Fu, B. 2018 Understanding the impacts of climate and land use change on water yield. *Current Opinion in Environment Sustainability* **33**, 167–174.

Zou, Y. & Mao, D. 2021 Analysis of water yield service of Lianshui River Basin in China based on ecosystem services flow model. *Water Supply*. ws2021265. https://doi.org/10.2166/ws.2021.265

First received 12 September 2021; accepted in revised form 2 December 2021. Available online 14 December 2021